Applications of Fluorescence in the Biomedical Sciences, pages 545–566
© 1986 Alan R. Liss, Inc.

27 Flow Cytometric Analysis of Endocytic Pathways

Robert F. Murphy and Mario Roederer

Receptor-mediated endocytosis is responsible for the uptake of many cellular proteins, hormones, toxins, and viruses [for reviews see Goldstein et al., 1979; Helenius et al., 1983; Pastan and Willingham, 1983]. Although there is evidence that all follow a common pathway into the cell [e.g., Maxfield et al., 1978], subsequent processing steps result in the differential sorting, degradation, and recycling of ligands and receptors. A number of studies on virus [Helenius et al., 1980; Miller and Lenard, 1980; Yoshimura et al., 1982; Marsh et al., 1983] and toxin [Sandvig and Olsnes, 1980; Draper and Simon, 1980; Marnell et al., 1982; Boquet and Duflot, 1982] endocytosis demonstrate a crucial role of the acidification of these ligands in their infectious mechanisms. Endosome acidification has also been demonstrated to play a role in recycling of some receptors [Tietze et al., 1980; Gonzalez-Noriega et al., 1980; Van Leuven et al., 1980].

Fluorescent measurements of the pH of compartments involved in endocytosis were first performed by Ohkuma and Poole [1978]. Using a fluorometer, they measured the excitation spectrum of cells containing fluorescein isothiocyanate (FITC)-dextran, and showed that the ratio of fluorescence emission resulting from excitation at 450 nm and 490 nm was proportional to pH. We have used fluorescein-labeled ligands and flow cytometry to demonstrate that the acidification process occurs much more rapidly than had previously been thought [Murphy et al., 1982a,b]. Tycko and Maxfield

Department of Biological Sciences, Center for Fluorescence Research in Biomedical Sciences, Carnegie-Mellon University, Pittsburgh, Pennsylvania 15213.

presented evidence that alpha-2-Macroglobulin is acidified before it enters lysosomes [Tycko and Maxfield, 1982].

In contrast to many ligands which are rapidly degraded in lysosomes, transferrin is not appreciably degraded by some cell types. Van Renswoude et al. [1982] demonstrated that transferrin-containing vesicles are nonetheless mildly acidified. Using dual fluorescence flow cytometry, we have demonstrated two phases of acidification of insulin by 3T3 cells [Murphy et al., 1984a]; these may correspond to entry into the mildly acidic, transferrin-containing compartment followed by transfer to lysosomes. Epidermal growth factor (EGF) has been demonstrated to be degraded in lysosomes [Carpenter and Cohen, 1979]; however, at least some EGF is internalized into nonlysosomal vesicles [Miskimmins and Shimizu, 1984]. Mellman and co-workers [Mellman et al., 1984; Mellman and Plutner, 1984] have demonstrated that complexes formed by monovalent, but not polyvalent, antibodies against the macrophage Fc receptor are recycled. This recycling may occur before acidification takes place.

Taken together, these data on whole cells for a variety of cell types and a number of ligands indicate that at least two types of endocytic compartments may be acidic, and that some receptor-ligand complexes (e.g., those involving transferrin and monovalent antibodies to Fc receptor) may be endocytosed and recycled without encountering lysosomes. This separation into at least two compartments is strongly supported by the data of Galloway et al., [1983], who found that two distinct, FITC-dextran-containing fractions isolated on Percoll gradients were capable of acidifying their contents in vitro in the presence of ATP. To complicate the acidification picture, both fractions of clathrin-coated vesicles [Forgac et al., 1983] and Golgi vesicles [Glickman et al., 1983] have also been demonstrated to contain proton pumps. In addition, at least two types of endosomes may exist: "light" endosomes (primary endocytic vesicles?) and "heavy" endosomes [Merion and Sly, 1983].

Despite significant progress during the past 5 years, a number of questions regarding endocytosis have been only partially answered. What is the pH of the initial compartment? What are the kinetics of acidification at different temperatures? Is the initial acidification process passive (ion antiport) or active (proton pump)? Do all ligands follow the same initial pathway of internalization, and at what point do they diverge?

Flow cytometry is ideally suited for answering these questions, for several reasons: (1) It allows measurement of more than one parameter (variable) simultaneously. These include intrinsic (cell volume, light scattering at various angles) and extrinsic (fluorescence of labeled probes) parameters. (2) Measurements can be made on a cell-by-cell basis on viable cells, so that physiological variables such as pH can be measured and the correlations

between measured parameters can be determined. (3) Data for large numbers of cells can be collected rapidly. Thus, statistically significant results may be obtained even on very heterogeneous samples. (4) Subpopulations of cells may be physically isolated by flow sorting for further microscopic or biochemical analysis.

We have undertaken a series of experiments to address the questions listed above, and in the process have developed new techniques for the analysis of cell systems by flow cytometry. In particular, we have devised methods for (1) correcting for autofluorescence in low signal-to-noise systems, (2) acquiring temporally resolved data yielding high-resolution kinetics of processes such as binding, internalization, and acidification of a fluorescent ligand, (3) obtaining the temperature dependence of these processes, and (4) analyzing subcellular components, such as endosomes and lysosomes, in unfractionated cell lysates.

AUTOFLUORESCENCE CORRECTION

Analysis of peptide receptors by using fluorescent techniques is often complicated by high levels of autofluorescence from unlabeled cells, most of which can be attributed to pyridine and flavin nucleotides [Aubin, 1979; Benson et al., 1979.] The amount of autofluorescence of a typical 3T3 cell is equivalent to 35,000 molecules of fluorescein; thus, when working with ligands such as FITC-EGF, of which only 21,000 bind to a cell, autofluorescence is a major portion of the signal. A wide variation in cell size is often observed in cultured cells such as fibroblasts. This variation can affect both the number of receptors and the autofluorescence, and can be large enough that a small cell with a number of ligands bound can show less fluorescence than a large unstained cell. We have devised a method for reducing the error due to autofluorescence by using either light scattering or a second wavelength "autofluorescence" emission to normalize for cell size. The basic procedure is illustrated in Figure 1.

Monolayers (60 mm) of 3T3 cells were washed twice with phosphate-buffered saline (PBS); 0.5 ml of Dulbecco's modified Eagle's medium (DMEM) was added. After 10 min, FITC-EGF was added to one plate to a concentration of 10 nM, to another, it was added to 10 nM along with 325 nM unlabeled EGF. This concentration of unlabeled EGF should reduce the binding of labeled EGF by 94%. After 30 min at 37°C, the cells were washed twice with PBS and trypsinized for 5 min at 37°C. These samples were then run on the fluorescence-activated sorter (FACS) and analyzed for forward scatter, right-angle scatter, and fluorescence at 530 nm [*F*(488,530), FITC] and 625 nm [*F*(488,625), autofluorescence] when excited by an argon laser

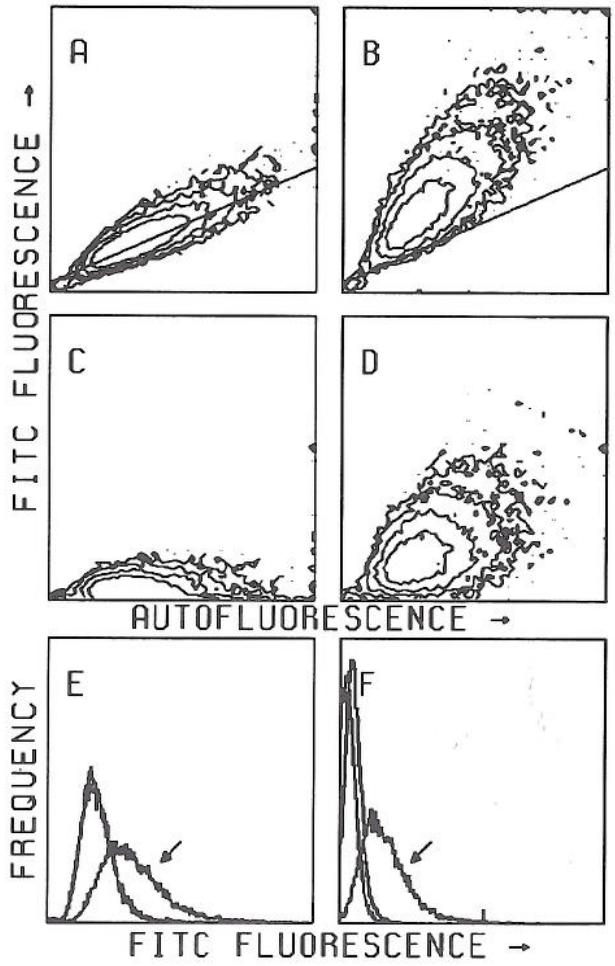

Fig. 1. Autofluorescence correction method. A–D. Dual parameter histograms are shown for two samples: control cells (A,C) and cells incubated with FITC-EGF as described in the text (B,D). Contours are drawn at 2, 6, 18, and 48 cells. Panel A shows the correlation between autofluorescence at 530 nm and 625 nm for the unstained cells. The line shows the best-fit line relating these parameters. The slope of this line predicts the proportion of 625 fluorescence which will be present in the 530 signal, regardless of whether "real" 530 fluorescence is present. Panel B demonstrates that most of the labeled cells are above this line. By correcting for autofluorescence (see text), the control distribution is shifted down to the horizontal axis, and the vertical axis becomes "real" 530 fluorescence (C,D). E–F. Single-parameter histograms are shown for the uncorrected (E) and corrected (F) F(488,530) of three samples each. The three histograms are: control cells, cells plus FITC-EGF (arrows), and cells plus FITC-EGF plus a 32-fold excess of unlabeled EGF (30-min incubations at 37°C). (The histograms for the control and blocked samples are almost identical.) Note the much smaller overlap between the control and the labeled samples in the corrected (right) histograms compared with the uncorrected histograms.

istograms are shown for
F as described in the text
the correlation between
e line shows the best-fit
oportion of 625 fluores-
"real" 530 fluorescence
e this line. By correcting
n to the horizontal axis,
Single-parameter histo-
) of three samples each.
s), and cells plus FITC-
37°C). (The histograms
much smaller overlap
tograms compared with

at 488 nm; 10,000 live cells (selected by thresholding on forward scatter) were analyzed for each sample.

Because autofluorescence of cultured cells shows wide excitation and emission spectra [Aubin, 1979; Benson et al., 1979], it is possible, with appropriate optical filters, to analyze a sample of cells and collect a parameter containing only autofluorescence. In this example, in which the probe is FITC-EGF the autofluorescence is detected by a bandpass filter at 625 nm with a bandwidth of 35 nm. There is little detectable fluorescein fluorescence within this band, so all signal is due to autofluorescence (data not shown).

In order to correct for the amount of autofluorescence in the 530-nm-band signal, therefore, only one assumption need be made: that the autofluorescence at 625 nm is proportional to the autofluorescence at 530 nm. To obtain this constant of proportionality, a control cell sample (with no FITC-EGF) is analyzed (Fig. 1a). It is observed that a straight line with a slope of 0.454 and a correlation coefficient of 0.864 relates the emission at 530 nm to that at 625 nm, indicating that this assumption is valid. This slope was then used in subsequent experiments with FITC-EGF to correct for the autofluorescence. In particular, the amount of signal in the autofluorescence parameter was used to gauge the amount of autofluorescence in the fluorescence parameter:

$$F_{\text{real}} = F(488,530) - F(488,625) \times S_{625,530}$$

where F_{real} is the amount FITC fluorescence which would have been observed in the absence of any autofluorescence, $F(488,530)$ and $F(488,625)$ are the measured fluorescence values as described above, and $S_{625,530}$ is the spillover between them calculated from the control (in the example $S_{625,530} = 0.454$). This calculation was done on a cell-by-cell basis (on list-mode data using the CALC4 program we have developed) for the samples containing FITC-EGF; the results for all cells were combined to obtain corrected histograms (Fig. 1E,F), means, and percent positives (Table 1). The success of the correction is shown by the reduced overlap between the histograms and the increase in percent positive from 48% to 84%.

The degree to which noise is reduced should be related to the correlation between the actual autofluorescence at 530 nm and the parameter being used to estimate it in the control sample. For instance, if we compare forward-angle scatter, right-angle scatter, and $F(488,625)$ as a measure of the autofluorescence at 530 nm, then we expect the correction to be the best using $F(488,625)$, followed by side scatter, with the least correction being obtained with forward scatter (see Table 1 for correlation coefficients). The order of the latter two comes from the expected correlation of autofluorescence with

TABLE 1. Autofluorescence Correction

Parameter used for correction	Correlation with *F* (488,530)	% positive[1]	Coefficient of variation (%)	
			Control	FITC-EGF[2]
None	N/A	48.5	38	41
Forward scatter	0.236	58.7	33	37
Side scatter	0.452	70.0	20	30
F (488,625)	0.864	84.4	29	35

[1]Number of cells which exceed a threshold selected to eliminate 95% of the appropriate unlabeled control sample.
[2]FITC, fluorescein isothiocyanate; EGF, epidermal growth factor.

cell size, which is better reflected by side scatter. In Table 1, we see that this order is reflected in the percent positive after correction.

ON-LINE KINETICS

Until recently, the data obtained by flow cytometry normally was from static populations; any active processes were stopped in order to acquire statistically significant data. Martin and Swartzendruber [1980] first included a measure of elapsed time as another parameter in flow cytometry. Previously, kinetic information was obtained only by multiple discrete measurements. These authors discuss the disadvantages of this technique, and demonstrate the increased accuracy in the determination of rapid kinetics by including time as a parameter. As opposed to making time an actual parameter for every cell, we have developed a system which continuously acquires data from the cytometer, on a cell-by-cell basis, and also records the number of cells analyzed during fixed intervals from 1/60 sec to 60 min [McNeil et al., 1985; Roederer and Murphy, in preparation]. Usually, intervals of 1 sec are used. Here we show two illustrations of the use of this system. First, we have used the method to ascertain the kinetics of the acidification of internalized insulin. Secondly, we have measured the kinetics with which endocytosed fluid is delivered to proteolytically active compartments.

Insulin Acidification Kinetics

Figure 2 shows the binding, internalization, and acidification of FITC- and tetramethyl rhodamine isothiocyanate (TRITC) insulin by 3T3 fibroblasts. Cells were suspended by scraping and additions were made directly to the cell suspension (see legend). Because the sample is being run continuously on the sorter, the amount of fluorescence per cell is measured as a function of time for the whole population. Thus, by averaging the measured

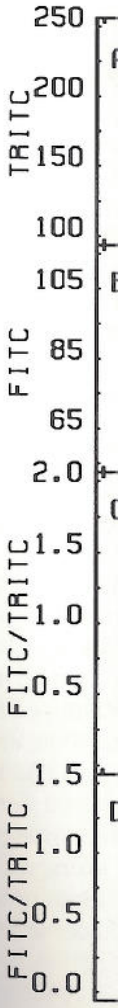

Fig. 2. Binding, i
twice with PBS a
to obtain autoflu
added to the samp
After the amount
A,B. Uncorrecte
function of time.
over 1 (C)- or 10
the ratio of the re

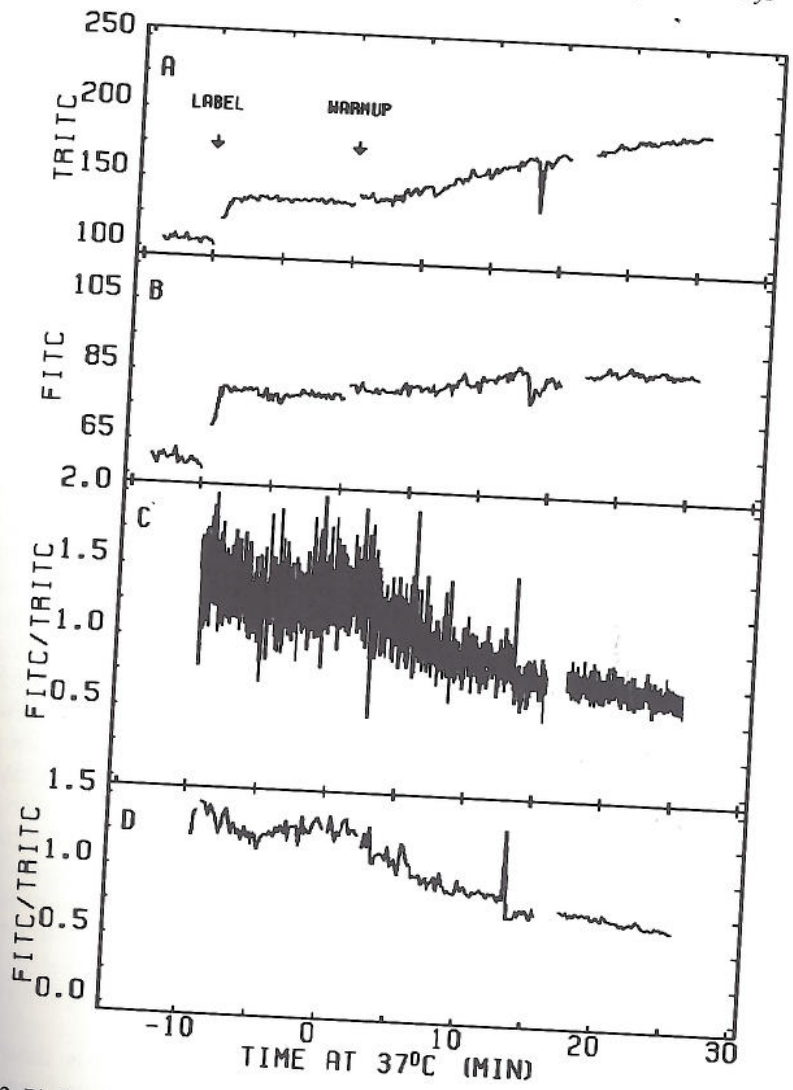

Fig. 2. Binding, internalization, and acidification of insulin. 60-mm monolayers were washed twice with PBS and then scraped into PBS. After 10 min on ice, they were run on the FACS to obtain autofluorescence levels for both red and green. FITC- and TRITC-insulin were added to the sample while it was still on ice [time of addition marked with an arrow in (A)]. After the amount of binding had stabilized, the cells were warmed to 37°C (second arrow). A,B. Uncorrected fluorescent signals for FITC-insulin (A) and TRITC-insulin (B) as a function of time. C,D. These plots were obtained by averaging the two fluorescent signals over 1 (C)- or 10 (D)-sec periods, subtracting out the average autofluorescences, and taking the ratio of the resulting FITC value to the TRITC value.

parameters over short periods of time (between 1 and 10 sec, or about 200 and 2,000 cells per period, respectively) to eliminate a large part of statistical noise, the internalization of the fluorescent ligand is observed as a function of time on a resolution of 1 or 10 seconds.

By subtracting the autofluorescence and then taking the ratio of the FITC and TRITC signals, a value proportional to the pH in which the ligand is found is obtained. Several features are evident in Figure 2: (1) binding is complete within 1 to 2 min of labeling; (2) a continuous and linear uptake of TRITC-insulin is observed after warmup; (3) a small increase in the FITC signal is observed, resulting in a ratio which steadily declines from roughly 1.5 to 0.7 over 30 min. This corresponds in a pH change from 7.4 to about 6.1. Since the amount of surface-bound ligand remains constant (confirmed by trypsinization; data not shown), we expect only a small increase in the FITC signal after warmup, since the fluorescence which would result from internalized ligand is rapidly quenched by acidification.

As was originally described by Bohn [1976] and discussed in detail by Murphy [1986], in flow cytometry the fluorescence from unbound ligand is usually negligible compared to that observed from the labeled cell (for appropriate numbers of receptors and high enough affinity ligands). However, two problems arise in analyzing steps subsequent to binding. First, there can be as much as one surface complement of ligand on the membrane which is not acidified. Thus, to obtain internal pH, corrections must be made for the amount of surface-bound ligand. This amount can be determined from parallel samples at fixed time points by using either trypsinization or pH shifts (for fluorescein-conjugated ligands; Finney and Sklar [1983]). With this information, the total fluorescence observed can be corrected for the surface complement. Second, there is also a distribution of ligand throughout the endocytic compartments, and a calculated pH will be the average of all compartments in which the ligand is found throughout the cell. Both of these problems can be partially overcome by using a pulse-chase protocol in which the processing of ligand can be expected to be synchronized.

MNA-Peptide Hydrolysis

Another example of the acquisition of on-line kinetics data is shown in Figure 3. In order to measure the kinetics with which endocytosed material is degraded, a fluorogenic enzyme subtrate, N-carbobenzyloxy-ala-arg-arg-4-methoxy-β-naphthylamine (MNA-peptide), was used [Murphy, Bowser, and Roederer, in preparation]. The basis for the assay has been described by Dolbeare and Smith [1977] and Dolbeare and Vanderlaan [1979]. Briefly, the free MNA resulting from enzymatic digestion of the MNA-peptide reacts with 5-nitrosalicylaldehyde (NSA) to form an insoluble product with an emission maximum near 530 nm. By measuring MNA-NSA fluorescence as a function of time after additon of MNA-peptide, we can determine the

earliest point at which endocytosed fluid reaches a compartment in which proteolytic enzymes are found.

A subconfluent 60-mm monolayer culture was used for each sample. The medium was removed, the cells were quickly washed twice with PBS, and the cells were removed by scraping with a rubber policeman in 2.9 ml of PBS. These unlabeled cells were then analyzed on the FACS for 2–5 min (at the appropriate temperature, see below), to determine an autofluorescence "baseline." The sample was removed from the FACS, MNA-peptide (0.5 mM) and NSA (1 mM) were added (in the presence or absence of inhibitors as described below), and analysis was continued. The sample temperature was maintained by a circulating water bath during acquisition. To control for nonspecific hydrolysis of the substrate and fluorescence resulting from NSA alone, proteinases were inhibited by the addition of leupeptin immediately before the addition of MNA-peptide and NSA. To control for uptake and/or hydrolysis by nonendocytic processes (e.g., secretion of enzymes into media, cell lysis, or diffusion through the plasma membrane), endocytosis was inhibited by using cytochalasin B [Wagner et al., 1971]. In this case, cells were incubated in cytochalasin B for 20 min at 37°C before scraping and addition of NSA and MNA-peptide.

As is shown in Figure 3, hydrolysis of MNA-peptide begins almost immediately after its addition to cells, and continues linearly for at least 35 min. The vast majority of this hydrolysis is due to enzymatic cleavage, since 95% can be inhibited by coincubation with leupeptin; most is also dependent on endocytosis, since 86% is inhibited when cells are preincubated with cytochalasin B. The kinetics of appearance of the MNA-NSA fluorescence thus provides an excellent reflection of the kinetics with which endocytosed fluid reaches a compartment containing protease.

Since these measurements were made in the continual presence of 1 mM NSA, the rate of cleavage observed may not reflect the rate which would be observed in the absence of NSA. We are currently investigating the possibility of using direct UV excitation of the liberated MNA to eliminate this possibility.

COMPARISON OF ACIDIFICATION KINETICS FOR DIFFERENT LIGANDS

There is some disparity in the reports of the pH to which various ligands are internalized. To determine whether the initial kinetics of acidification are biphasic [Murphy et al., 1984a], the acidification of three fluorescent conjugates were analyzed by different methods. A summary of these results is shown in Figure 4. For EGF, FITC-EGF was added to 10 nM; the cells were incubated for various periods, trypsinized, and analyzed by using the amine-

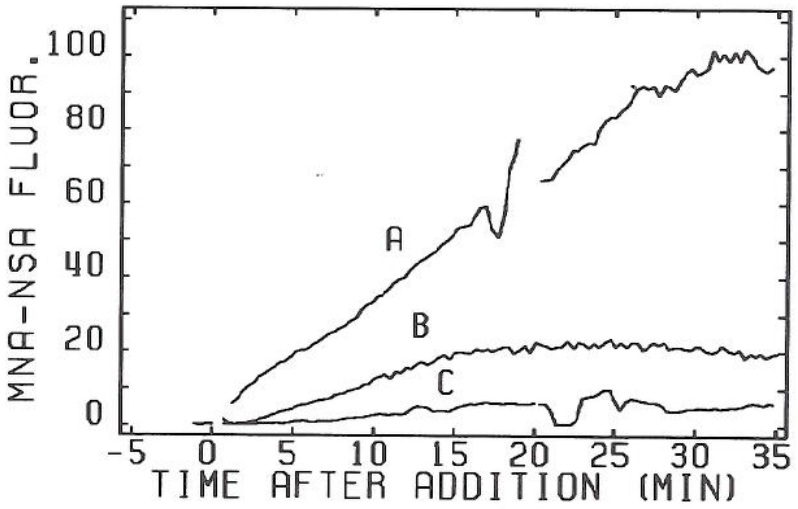

Fig. 3. MNA-peptide hydrolysis kinetics. Cells were scraped from tissue culture dishes at 0°C and run on the FACS at 37°C to obtain the background autofluorescence. MNA-peptide (Research Plus), NSA (Eastman Kodak), and either cytochalasin B (endocytosis inhibitor) or leupeptin (proteolysis inhibitor) or no inhibitor was added and the cells were analyzed during continuous incubation at 37°C. The fluorescence resulting from excitation at 488 nm was measured for each cell by using a 530-nm bandpass filter (30-nm bandwidth). A. Cells plus MNA-peptide and NSA. B. Cells incubated with 20 μg/ml cytochalasin B for 20 min, scraped, and run in MNA-peptide and NSA as in A. C. Cells plus MNA-peptide, NSA, and 100 μg/ml leupeptin; 86% of the hydrolysis is due to postendocytic enzymatic cleavage, since 5% is not blocked by leupeptin and an additional 9% (a total of 14%) is not blocked by cytochalasin B.

ratio method [Murphy et al., 1982a]. The EGF went through only one round of internalization as demonstrated by a constant level of signal (after methylamine addition) independent of incubation time (data not shown); thus, it enters the endocytic pathway synchronously and provides a signal equivalent to a pulse-chase experiment. For insulin, both FITC- and TRITC-insulin were added simultaneously to a concentration of 100 nM as shown above in Figure 2. The labeled insulins were taken up linearly with time (data not shown). Finally, FITC-and XRITC-dextran were added simultaneously to monolayers to a concentration of 1 mg/ml. After a 5-min incubation at 37°C, the cells were washed 8 times with PBS, and incubation continued for various periods of time in media at 37°C. pH calculations were done as follows: for EGF, autofluorescence was subtracted from the average fluorescein signal before and after the addition of methylamine. This ratio was compared to a pH calibration performed on a fluorometer to obtain a value corresponding to the pH in which the FITC-EGF was found. The background for insulin

was determined by binding insulin to cells at 0°C. This represents autofluorescence plus the signal due to surface-bound insulin. This value was subtracted from the subsequent incubation samples to obtain a value for internal fluorescence. The ratio of the background-corrected fluorescein and rhodamine signals was compared to a pH calibration curve to obtain an average pH of internal insulin. Because ligand was continuously present, the resulting pH is an average for ligand throughout the endocytic pathway, and is expected to be higher than that for ligand that has synchronously entered the cells. The dextran pH was calculated by subtracting autofluorescence, taking the ratio of the fluorescein and rhodamine signals, and comparing to a dextran calibration curve for that experiment.

Figure 4 shows the close correlation between the pH calculated for dextran and EGF and the slightly higher values obtained for insulin. All three ligands demonstrate a rapid acidification to approximately pH 6.0 (within 5 min of labeling), followed by a slow acidification to a pH as low as 5.2 (50 min with EGF). A previous report comparing the pH to which alpha-2-macroglobulin and transferrin are acidified [Yamashiro et al., 1984] suggests that

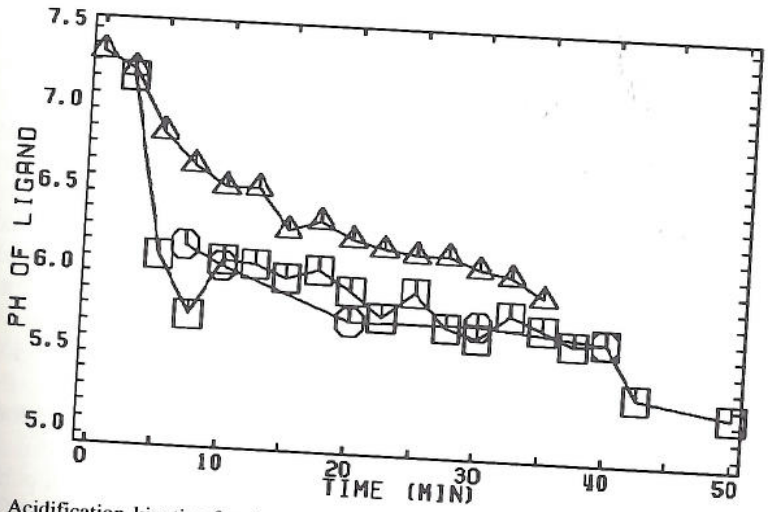

Fig. 4. Acidification kinetics for dextran, insulin, and EGF. Swiss 3T3 cells were incubated continuously with either 10 nM FITC-EGF (□) or 100 nM FITC- and TRITC-insulin (Δ), or pulsed for 5 min with 1 mg/ml FITC- and XRITC-dextran and chased (○). The average pH at which ligand is found is plotted as a function of time after addition of the label. Note the close overlap between the EGF and the dextran curves. The insulin curve shows a slightly higher average pH, since the continuous incubation procedure yields an average over all compartments. Although EGF was also present in a continuous incubation, the ligand was synchronously endocytosed in the time frame of this experiment (see text), and thus resembles a pulse-chase experiment.

the initial pH is ligand-dependent. It was reported that FITC-transferrin was acidified to pH 6.4 within 10 min, and that it was not acidified to a lower pH. FITC-α_2-macroglobulin, on the other hand, was rapidly acidified to either pH 5.4 $\pm$ 0.1 [Yamashiro et al., 1984] or pH 5.0 $\pm$ 0.2 [Tycko and Maxfield, 1982] and was not further acidified, even when delivered to lysosomes. However, we found that the initial pH to which insulin was acidified was higher (approximately pH 6) than that which it eventually reached (approximately pH 5) [Murphy et al., 1984a]. Biphasic acidification kinetics were also observed for antibodies directed against H-2K [Murphy et al., 1984b]. The evidence in Figure 4 demonstrates that at least these three ligands are intially exposed to pH 6 and then (possibly) later to a lower pH. This explains the observation (A. Helenius, personal communication) that the Semliki Forest virus (SFV) fus-1 mutant (which requires a pH of 5.5 for infection [Kielian et al., 1984]) requires at least 45 min at 20°C to infect while the wild-type virus can infect in less than 5 min.

TEMPERATURE DEPENDENCE OF ACIDIFICATION

From the in vitro data of Galloway et al. [1983], the mechanism of endosome acidification in vivo would appear to be through an ATP-requiring proton pump. This conclusion is supported by the data of Maxfield [1982] and Yamashiro et al. [1983]. These data are inconclusive, however, since (1) no evidence is presented in either paper that the probe is not contained in lysosomes; (2) the fluorescence values are not calibrated to allow accurate comparison either internally or with other papers (e.g., Fig. 2 of Maxfield [1982] and Fig. 1 of Yamashiro et al. [1983]); (3) the digitonin-"permeabilized" cells may not reflect the in vivo system. Additional experiments are required to firmly establish the active nature of this initial acidification step.

One means of examining the energy requirements for this initial acidification is to determine its temperature dependence. The temperature dependence of some of the steps in endocytosis has already been addressed by several groups. Some conflict exists, however, and no reliable information is available about the exact pH to which ligands are acidified at temperatures below 37°C. Internalization of ligand begins at approximately 10°C. For example, Pesonen et al. [1984] observed no uptake of ligand at 10°C, whereas Marsh et al. [1983] observed internalization of roughly 10% of the amount taken up at 37°C. By 15°C, 40% of the 37°C amount of ligand was internalized. Virus is capable of infecting cells at 15°C, demonstrating acidification at this temperature. Pesonen et al. [1984] found no transcytosis of G protein at 15°C, indicating that sorting may be blocked at this temperature. Oka and Weigel [1983] demonstrated that at 18°C an asialoglycoprotein

is found in two distinct compartments: one in which dissociation occurs, and one in which the the ligand remains complexed to the receptor. It was not ascertained whether this was due to sorting after internalization, or internalization of ligand into two different compartments.

Transcytosis of G protein does occur at 20°C, indicating that sorting of ligands occurs at this temperature. Galloway et al. [1983] demonstrated that FITC-dextran internalized at this temperature is found in endosomes that are capable of acidifying in vitro. Matlin and Simons [1983] found that hemagglutinin protein is not exocytosed at 20°C even 2 hours after its synthesis. There is evidence that part of the endocytic and exocytic pathways converge at the Golgi complex, and this experiment would indicate therefore that there is still a processing step blocked at 20°C. Hopkins and Trowbridge [1983] showed that, at 22°C, transferrin receptor-antibody complexes traverse several compartments to arrive in juxtanuclear multivesicular bodies. However, no degradation was observed at this temperature. Upon warming to 37°C, the receptor was immediately transferred to lysosomal compartments and degraded. Finally, at 25°C, degradation was observed for G protein [Pesonen et al., 1984] and viral proteins [Marsh et al., 1983], but not the EGF receptor [Stoscheck and Carpenter, 1984]. The EGF receptor is degraded at 37°C.

We have addressed the question of the temperature dependence of various steps in the endocytic pathway by labeling cells with FITC- and XRITC-dextran at various temperatures. Figure 5 shows typical results from these experiments [Roederer and Murphy, in preparation]. At 11°C, acidification does not occur until after 20 min, at which point it proceeds to pH 6.1. At temperatures between 17°C and 21°C, acidification to pH 6.1 proceeds fairly rapidly but does not proceed beyond that point, at least up to 40 min. At 25°C and 37°C, dextran is already at pH 6.1 at the earliest time point (2-min chase following a 5-min pulse); however, acidification continues to almost pH 5.5 at 40 min.

Figure 5 also shows the temperature dependence of exocytosis of the internalized dextrans. At 11°C, the amount of dextran remaining slowly decreases to 60%. At temperatures up to 21°C, this process occurs much more rapidly, but remains at 60% even at 40 min. At 25°C, however, the amount remaining begins to decrease below 60%, and at 37°C almost 70% of the internalized ligand is lost. This correlates well with the temperature dependence of ligand processing and sorting. Our conclusion is that at temperatures up to 21°C, internalized ligand reaches pH 6.1 within 30 min, while approximately 45% is lost by "reversible endocytosis" [cf. Storrie et al., 1984]. At higher temperatures, acidification proceeds rapidly to pH 6, and more slowly to pH 5.5 or below; more dextran is slowly lost due to a recycling pathway that depends on a fusion or processing event, possibly involving lysosomes.

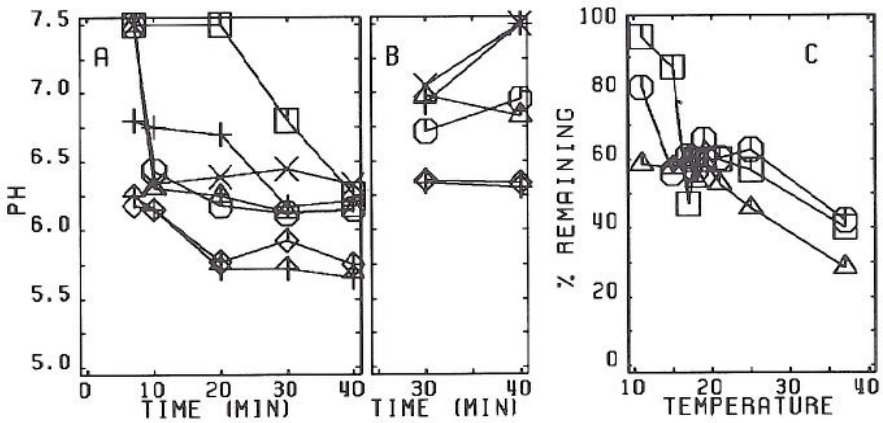

Fig. 5. Temperature dependence of dextran acidification and exocytosis. FITC- and XRITC-dextran were added to cells on tissue culture plates at a concentration of 1 mg/ml for 5 min; the cells were washed extensively with PBS and medium was added for the duration of the chase. All operations were carried out with solutions and cells equilibrated in a refrigerated water bath with the temperature held to within 0.1°C. A. The pH of the compartments containing dextran as calculated according to the text is plotted as a function of time after addition of dextran for cells incubated at 11°C (□), 17°C (○), 18°C (Δ), 19°C (+), 21°C (×), 25°C (◇), and 37°C (↑). B. The pH of the cellular compartments after neutralization with 200 mM methylamine for 5 min at 24°C (symbols as in A). C. The amount of XRITC-dextran remaining in the cell after 20 min (□), 30 min (○), and 40 min (Δ) after addition of dextran, relative to the amount present at the earliest time point (5-min pulse, 2-min chase) is shown as a function of temperature of incubation. At low temperatures, there is a slow loss of ligand to 60% of the initial value. The intermediate temperatures show a rapid loss to 60%, while the warm temperatures show an additional loss to less than 40% of the initial amount.

A distinction between the endosomal and lysosomal compartments can also be made by examining the extent of neutralization by 200 mM methylamine of these compartments (Fig. 5B). The low-temperature samples were neutralized to pH 7.0–7.5, whereas the 25°C and 37°C samples were only neutralized to pH 6.5. Because the neutralization was done at the same temperature (24°C) for all samples, the difference in final pH is not a consequence of temperature sensitivity of the acidification mechanism but rather of the fact that at the lower temperatures, ligand is not delivered to compartments that acidify as actively.

From Arrhenius plots (the natural logarithm of the amount of dextran taken up at the earliest time point versus inverse absolute temperature), we can obtain an energy of activation for the initial internalization step. By linear regression, we obtain an energy of activation of 8.8 kcal/mol (correlation

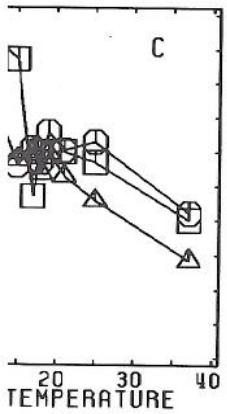

sis. FITC- and XRITC-
of 1 mg/ml for 5 min;
for the duration of the
brated in a refrigerated
d of the compartments
function of time after
(Δ), 19°C (+), 21°C
nts after neutralization
The amount of XRITC-
in (Δ) after addition of
pulse, 2-min chase) is
, there is a slow loss of
w a rapid loss to 60%,
of the initial amount.

compartments can
200 mM methylam-
ture samples were
samples were only
done at the same
final pH is not a
on mechanism but
is not delivered to

amount of dextran
mperature), we can
on step. By linear
al/mol (correlation

coefficient 0.947), a value less than half that observed previously. Measurements of 17–25 kcal/mol [Mahoney et al., 1977] and 19.5 kcal/mol [Kaplan and Nielsen, 1979] were obtained for the energy of activation of internalization by macrophages, 26.5 kcal/mol was obtained for perfused rat liver cells [Dunn et al., 1980], and 17.6 kcal/mol obtained for fibroblast internalization [Steinman et al., 1974]. Since previous measurements have used long (at least 30 min) incubations or warmup protocols which are not appropriate for this analysis, the value of 8.8 kcal/mol should be more accurate reflection of the activation energy of the initial endocytic event.

FLOW CYTOMETRIC VESICLE ANALYSIS

As discussed above, a great deal of information about the pathways of endocytosis has been obtained by using a combination of electron microscopy and traditional biochemical techniques. However, some of the details of these pathways are not yet known due to the limitations of the methods used. For example, morphological studies by electron microscopy have the advantage that spatial and structural information may be obtained. However, the method is inherently static, sample sizes are ordinarily limited, and it is difficult to quantitate enzymatic and biochemical properties. Density gradient centrifugation has been useful due to the possibility of performing biochemical analyses on the resulting fractions. However, the length of time required for fractionation introduces the possibility or changes in vesicle properties, as might be expected from proteolysis or loss of ion gradients. In addition, bulk fractionation techniques are unable to address questions which require particle-by-particle analysis, such as whether different endocytic probes or different enzymes are contained in the same compartment.

While the usefulness of flow cytometry for the study of endocytosis has been demonstrated previously [Murphy et al., 1982a, 1984a,b; Finney and Sklar, 1983], it has heretofore been limited mainly to measurements on whole cells. Geisow et al. [1982] have described a flow cytometric assay for extracellular fusion of lysosomes and phagosomes containing 5-μm latex spheres (phagosomes were detected by light scattering from the incorporated sphere; no attempt was made to detect the unfused lysosomes directly). Flow microfluorometric analysis of synthetic phosphatidylcholine/cholesterol vesicles has been described recently by Allen et al. [1984]. We have recently demonstrated the feasibility of using flow cytometry and sorting to characterize unfractionated cell lysates after labeling with endocytic and enzymatic probes [Murphy, 1985]. This technique offers the advantages of rapid measurement of large numbers of individual vesicles, the ability to simultane-

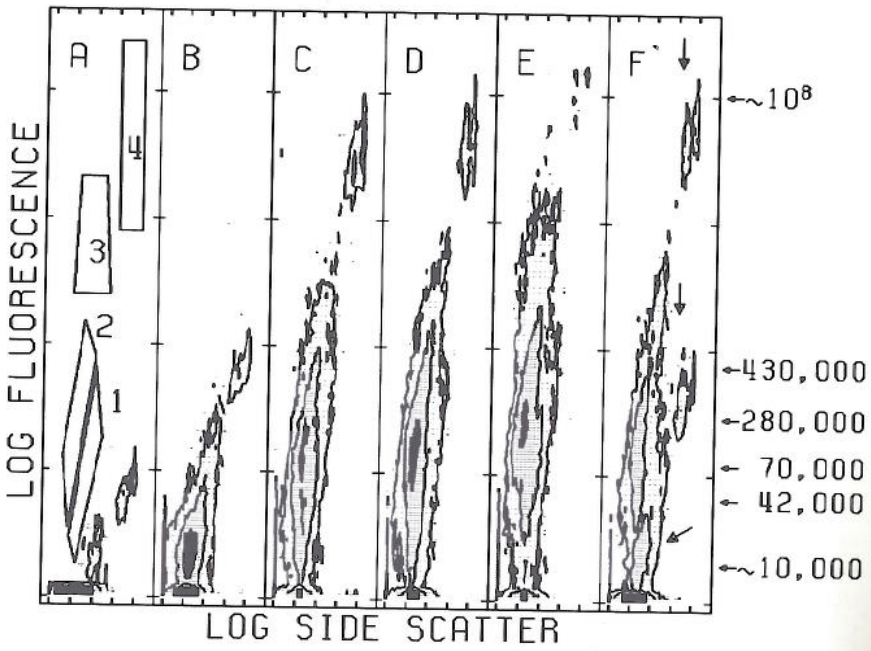

Fig. 6. Detection of endocytic vesicles by using flow cytometry. Crude cell lysates were prepared from control cells which did not receive any FITC-dextran (A), and from cells which were incubated with 50 mg/ml FITC-dextran for 5 sec (B), 20 min (C), 60 min (D), and 180 min (E). Each panel represents 50,000 events. The polygons in A show the regions in C–E where vesicles which show weak (1), intermediate (2), and bright (3) fluorescence are found. The position of intact fluorescent cells (4) is also shown. The arrows show the average fluorescence of four types of calibration microspheres, and two extrapolated values. A mixture of equal volumes of the samples in A and D was also analyzed (F). Note the presence of a population of unlabeled vesicles and two populations of intact cells in this mixture (large arrows). Contours are drawn at 3, 20, and 80 events per bin. Tics are placed at approximately one-log intervals.

ously measure more than one vesicle property, and the possibility of sorting individual vesicles for further analysis.

Primary effort in the area of vesicle analysis has thus far been directed to developing a flow cytometric procedure for analyzing individual endocytic vesicles in cell lysates [Murphy, 1985]. Some of the results of this analysis are shown in Figures 6 and 7. The results indicate that at least three kinetically distinct compartments may be identified by flow cytometry; these may correspond to light endosomes, heavy endosomes, and lysosomes. Figure 7 demonstrates the increased resolution of these populations obtained by normalizing the data by using light scatter.

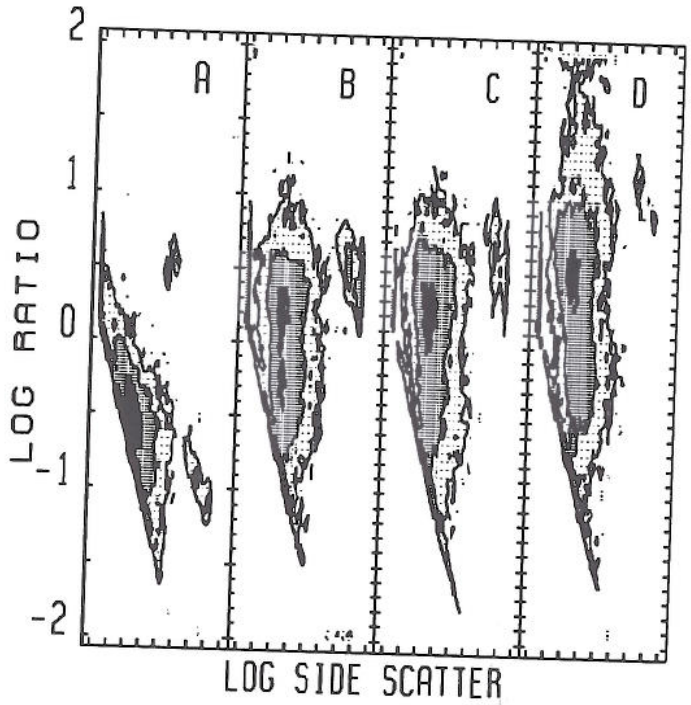

Fig. 7. Detection of endocytic vesicles in flow cytometry: correction for vesicle size. Panels A–D correspond to panels B–E in Figure 6. Plotted are dual-parameter histograms of the ratio of fluorescence to side scatter versus side scatter. Two populations are evident in panel B (20-min incubation with FITC-dextran); in panel D (180 min) a third highly fluorescent population at about 1.5 log units becomes apparent. Normalizing by this parameter reduces the variation in the fluorescent signal due both to differences in the position of the vesicle within the measuring beam (hydrodynamic focusing of vesicles is expected to be poorer than for the much larger cells for which flow cytometers are designed) and to differences in size of the individual vesicles; the resulting populations are more homogeneous and better separated from each other.

A 20-min incubation with FITC-dextran resulted in two distinct labeled populations. Merion et al. [1983] have demonstrated a similar resolution of at least two endocytic compartments after a 15-min incubation with FITC-dextran with Percoll gradients. As incubation time increases, a highly fluorescent population appears. The kinetics of the appearance of this population suggest that it may consist of secondary lysosomes and multivesicular bodies.

This approach has been combined with the use of the MNA-conjugated fluorogenic cathepsin B substrate described above to permit detection of compartments containing this proteolytic enzyme (Fig. 8). Correlation of the

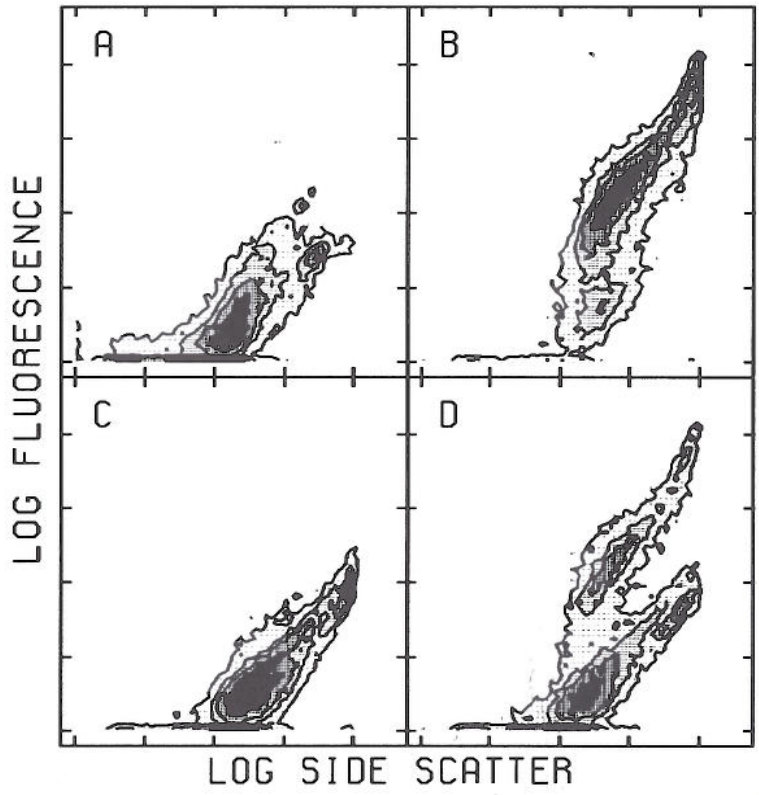

Fig. 8. Detection of vesicles containing cathepsin B activity. Flow cytometric analysis of lysates from cells incubated with (B,C) or without (A) fluorogenic substrate and with (C) or without (A,B) 100 μg/ml leupeptin. A mixture of equal volumes of the samples shown in B and C was also analyzed (D). The presence of both labeled and unlabeled populations in D demonstrates that the fluorescence is intravesicular. Contours are drawn at 5, 20, 40, and 80 events per bin. Tics are placed at approximately one-log intervals.

presence of endocytic markers with the presence of lysosomal enzymes should be possible by using this technique.

CONCLUSION

We have developed several new flow cytometric techniques for the analysis of endocytosis. First, by correcting for autofluorescence by using correlated parameters, the statistical significance of results with low signal-to-noise ratios is increased dramatically. This is crucial in many ligand systems where

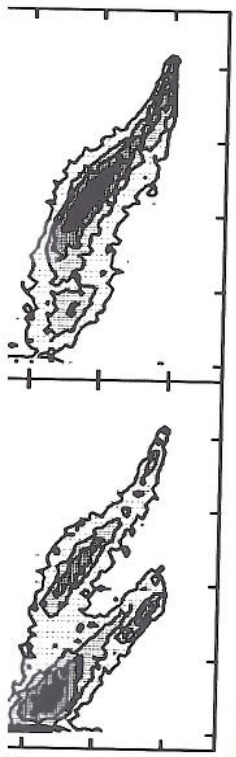

R

. Flow cytometric analysis of
genic substrate and with (C) or
ies of the samples shown in B
nd unlabeled populations in D
are drawn at 5, 20, 40, and 80
als.

of lysosomal enzymes

chniques for the analysis
ence by using correlated
vith low signal-to-noise
ny ligand systems where

less than 30,000 ligands bind to a cell. We have also demonstrated the usefulness of acquisition of real-time data on the flow cytometer. This allows the observation of kinetic processes with half-times on the order of seconds or minutes. We have used this system to analyze the kinetics with which pinocytosed ligand is acidified and delivered to degradatory compartments.

Additional experiments on other ligands demonstrate that ligand acidification is biphasic; in particular, both EGF and dextran are acidified to pH 6 within 5 min of internalization, followed by a slower acidification to pH 5.2 over the next 50 min. By varying the temperature of incubation, we have demonstrated that the second phase of this acidification is blocked below 21°C, but the first phase occurs even at 11°C.

Finally, we have used flow cytometry to analyze endocytic vesicles in unfractionated cell lysates. By analyzing large populations of vesicles labeled with fluorescent dextran, we have shown that there are three kinetically distinct compartments involved in endocytosis. Future experiments using these techniques should permit further elucidation of the biochemical properties of the compartments involved in endocytosis.

ACKNOWLEDGMENTS

We thank Amy Kennedy, Greg LaRocca, Robert Mays, and Daniel Shmorhun for technical assistance, and Robert Bowser, David Sipe, D. Lansing Taylor, and Alan Waggoner for helpful discussions. This work was supported in part by National Institutes of Health grant GM32508, and Presidential Young Investigator Award DCB-8351364 from the National Science Foundation, with matching funds from Becton Dickinson Monoclonal Center, Inc.

REFERENCES

Allen JK, Dennison DK, Schmitz KS, Morrisett JD (1984): Direct observation of the distribution of fluorescent probes in phosphatidylcholine/cholesterol vesicles using flow microfluorometry. Anal Biochem 140:409–416.

Aubin JE (1979): Autofluorescence of viable cultured mammalian cells. J Histochem Cytochem 27:36–43.

Benson RC, Meyer RA, Zaruba ME, McKhann GM (1979): Cellular autofluorescence—is it due to flavins? J Histochem Cytochem 27:44–48.

Bohn B (1976): High-sensitivity cytofluorometric quantitation of lectin and hormone binding to surfaces of living cells. Exp Cell Res 103:39–46.

Boquet P, Duflot E (1982): Tetanus toxin fragment forms channels in lipid vesicles at low pH. Proc Natl Acad Sci USA 79:7614:7618.

Carpenter G, Cohen S (1979): Epidermal growth factor. Ann Rev Biochem 48:193–216.

Dolbeare FA, Smith RE (1977): Flow cytometric measurement of peptidases with use of 5-nitrosalicylaldehyde and 4-methoxy-β-naphthylamine derivatives. Clin Chem 23:1485–1491.

Dolbeare F, Vanderlaan M (1979): A fluorescent assay of proteinases in cultured mammalian cells. J Histochem Cytochem 27:1493–1495.

Draper RK, Simon MI (1980): The entry of diphtheria toxin into the mammalian cell cytoplasm: Evidence for lysosomal involvement. J Cell Biol 87:849–854.

Dunn WA, Hubbard AL, Aronson NN (1980): Low temperature selectively inhibits fusion between pinocytic vesicles and lysosomes during heterophagy of ^{125}I-asialofetuin by the perfused rat liver. J Biol Chem 255:5971–5978.

Finney DA, Sklar LA (1983): Ligand/receptor internalization: A kinetic, flow cytometric analysis of the internalization of N-formyl peptides by human neutrophils. Cytometry 4:54–60.

Forgac M, Cantley L, Wiedenmann B, Altstiel L, Branton D (1983): Clathrin-coated vesicles contain an ATP-dependent proton pump. Proc Natl Acad Sci USA 80:1300–1303.

Galloway CJ, Dean GE, Marsh M, Rudnick G, Mellman I (1983): Acidification of macrophage and fibroblast endocytic vesicles *in vitro*. Proc Natl Acad Sci USA 80:3334–3338.

Geisow M, D'arcy Hart P, Young MR (1982): Extracellular fusion of macrophage phagosomes with lysosomes. Cell Biol Int Rep 6:361–367.

Glickman J, Croen K, Kelly S, Al-Awqati Q (1983): Golgi membranes contain an electrogenic H^+ pump in parallel to a Chloride conductance. J Cell Biol 97:1303–1308.

Goldstein JL, Anderson RGW, Brown MS (1979): Coated pits, coated vesicles, and receptor-mediated endocytosis. Nature 279:679.

Gonzalez-Noriega A, Grubb JH, Talkad V, Sly WS (1980): Chloroquine inhibits lysosomal enzyme pinocytosis and enhances lysosomal enzyme secretion by impairing receptor recycling. J Cell Biol 85:839–852.

Helenius A, Kartenbeck J, Simons K, Fries E (1980): On the entry of semliki forest virus into BHK-21 cells. J Cell Biol 84:404–420.

Helenius A, Mellman I, Wall D, Hubbard A (1983): Endosomes. Trends Biochem Sci 8:245–249.

Hopkins CR, Trowbridge IS (1983): Internalization and processing of transferrin and the transferrin receptor in human carcinoma A431 cells. J Cell Biol 97:508–521.

Kaplan J, Nielsen ML (1979): Analysis of macrophage surface receptors. J Biol Chem 254:7329–7335.

Kielian MC, Keranen S, Kaariainen L, Helenius A (1984): Membrane fusion mutants of semliki forest virus. J Cell Biol 98:139–145.

Mahoney EM, Hamill AL, Scott WA, Cohn ZA (1977): Response of endocytosis to altered fatty acyl composition of macrophage phospholipids. Proc Natl Acad Sci USA 74:4895–4899.

Marnell MH, Stookey M, Draper RK (1982): Monensin blocks the transport of diphtheria toxin to the cell cytoplasm. J Cell Biol 93:57–62.

Marsh M, Bolzau E, Helenius A (1983): Penetration of semliki forest virus from acidic prelysosomal vacuoles. Cell 32:931–940.

Martin JC, Swartzendruber DE (1980): Time: A new parameter for kinetic measurements in flow cytometry. Science 207:199–201.

Matlin KS, Simons K (1983): Reduced temperature prevents transfer of a membrane glycoprotein to the cell surface but does not prevent terminal glycosylation. Cell 34:233–243.

Maxfield FR (1982): Weak bases and ionophores rapidly and reversibly raise the pH of endocytic vesicles in cultured mouse fibroblasts. J Cell Biol 95:676–681.

Maxfield FR, Schlessinger J, Shecter Y, Pastan I, Willingham MC (1978): Collection of insulin, EGF, and α_2-macroglobulin in the same patches on the surface of cultured fibroblasts and common internalization. Cell 14:805–810.

McNeil PL, Kennedy AL, Waggoner AS, Taylor DL, Murphy RF (1985): Light-scattering changes during chemotactic stimulation of human neutrophils: Kinetics followed by flow cytometry. Cytometry 6:7–12.

Mellman I, Plutner H (1984): Internalization and degradation of macrophage Fc receptors bound to polyvalent immune complexes. J Cell Biol 98:1170–1177.
Mellman I, Plutner H, Ukkonen P (1984): Internalization and rapid recycling of macrophage fc receptors tagged with monovalent antireceptor antibody: Possible role of a prelysosomal compartment. J Cell Biol 98:1163–1169.
Merion M, Sly WS (1983): The role of intermediate vesicles in the adsorptive endocytosis and transport of ligand to lysosomes by humand fibroblasts. J Cell Biol 96:644–650.
Merion M, Schlesinger P, Brooks RM, Moehring JM, Moehring TJ, Sly WS (1983): Defective acidification of endosomes in chinese hamster ovary cell mutans "cross-resistant" to toxins and viruses. Proc Natl Acad Sci USA 80:5315–5319.
Miller DK, Lenard J (1980): Inhibition of vesicular stomatitis virus infection by spike glycoprotein. J Cell Biol 84:430–437.
Miskimins WK, Shimizu N (1984): Uptake of epidermal growth factor into a lysosomal enzyme-deficient organelle: Correlation with cell's mitogenic response and evidence for ubiquitous existence in fibroblasts. J Cell Physiol 118:305–316.
Murphy RF (1985): Analysis and isolation of endocytic vesicles by flow cytometry and sorting: Demonstration of three kinetically distinct compartments involved in fluid-phase endocytosis. Proc Natl Acad Sci USA 82:8523–8526.
Murphy RF (1986): Ligand binding, endocytosis and processing. In Melamed MR, Lindmo T, Mendelsohn ML (eds): "Flow Cytometry and Sorting," second edition. New York: John Wiley and Sons, in press.
Murphy RF, Jorgensen ED, Cantor CR (1982a): Kinetics of histone endocytosis in chinese hamster ovary cells. J Biol Chem 257:1695–1701.
Murphy RF, Powers S, Verderame M, Cantor CR, Pollack R (1982b): Flow cytofluorometric analysis of insulin binding and internalization by swiss 3T3 cells. Cytometry 2:402–406.
Murphy RF, Powers S, Cantor CR (1984a): Endosome pH measured in single cells by dual fluorescence flow cytometry: Rapid acidification of insulin to pH 6. J Cell Biol 98:1757–1762.
Murphy RF, Tse DB, Cantor CR, Pernis B (1984b): Acidification of internalized class I major histocompatibility complex antigen by T lymphoblasts. Cell Immunol 88:336–342.
Ohkuma S, Poole B (1978): Fluorescence probe measurement of the intralysosomal pH in living cells and the perturbation of pH by various agents. Proc Natl Acad Sci USA 75:3327–3331.
Oka JA, Weigel PH (1983): Recycling of the asialoglycoprotein receptor in isolated rat hepatocytes. J Biol Chem 258:10253–10262.
Pastan I, Willingham MC (1983): Receptor-mediated endocytosis: Coated pits, receptosomes, and the golgi. Trends Biochem Sci 8:250–252.
Pesonen M, Ansorge W, Simons K (1984): Transcytosis of the G protein of vesicular stomatitis virus after implantation into the apical plasma membrane of madin-darby canine kidney cells. I. Involvement of endosomes and lysosomes. J Cell Biol 99:796–802.
Sandvig K, Olsnes S (1980): Diphtheria toxin entry into cells is facilitated by low pH. J Cell Biol 87:828–832.
Steinman RM, Silver JM, Cohn ZA (1974): Pinocytosis in fibroblasts. J Cell Biol 63:949–969.
Storrie B, Pool RR, Sachdeva M, Maurey KM, Oliver C (1984): Evidence for both prelysosomal and lysosomal intermediates in endocytic pathways. J Cell Biol 98:108–115.
Stoscheck CM, Carpenter G (1984): Down regulation of epidermal growth factor receptors: Direct demonstration of receptor degradation in human fibroblasts. J Cell Biol 98:1048–1053.
Tietze C, Schlesinger P, Stahl P (1980): Chloroquine and ammonium ion inhibit receptor-mediated endocytosis of mannose-glycoconjugates by macrophages: Apparent inhibition of receptor recycling. Biochem Biophys Res Comm 93:1–8.

Tycko B, Maxfield FR (1982): Rapid acidification of endocytic vesicles containing alpha-2-macroglobulin. Cell 28:643–651.

Van Leuven F, Cassiman J-J, Van Den Berghe H (1980): Primary amines inhibit recycling of α_2-macroglobuline receptors in fibroblasts. Cell 20:37–43.

Van Renswoude J, Bridges KR, Harford JB, Klausner RD (1982): Receptor-mediated endocytosis of transferrin and the uptake of Fe in K562 cells: Identification of a nonlysosomal acidic compartment. Proc Natl Acad Sci USA 79:6186–6190.

Wagner R, Rosenberg M, Estensen R (1971): Endocytosis in chang liver cells. J Cell Biol 50:804–817.

Yamashiro DJ, Fluss SR, Maxfield FR (1983): Acidification of endocytic vesicles by an ATP-dependent proton jump. J Cell Biol 97:929–934.

Yamashiro DF, Tycko B, Fluss SR, Maxfield FR (1984): Segregation of transferrin to a mildly acidic (pH 6.5) para-golgi compartment in the recycling pathway. Cell 37:789–800.

Yoshimura A, Kuroda K, Kawasaki K, Yamashina S, Maeda T, Ohnishi S (1982): Infectious cell entry mechanism of influenza virus. J Virol 43:284–293.